

Inductively Coupled Plasma Reactor for High-Yield Carbon Vaporization  
and Generation of Vibrationally Excited CO in Reaction with Molecular Oxygen.

Thesis

Presented in Partial Fulfillment of the Requirements for Research Distinction  
in the Department of Mechanical and Aerospace Engineering.

By

Ilya Gulko

B. S. in Mechanical Engineering

The Ohio State University

2018

Thesis Committee

Dr. Igor V. Adamovich

Dr. William J. Rich

Copyrighted by

Ilya Gulko

2018

## Abstract

Recent work in the Nonequilibrium Thermodynamics Laboratories demonstrated that a chemical reaction between carbon atoms, generated in a high-temperature arc discharge with graphite electrodes, and molecular oxygen produces highly vibrationally excited CO. In these experiments, absolute population inversion among CO vibrational levels has been detected in a collision-dominated environment, suggesting feasibility of development of a novel CO chemical laser. This laser would be able to operate in a high-speed airflow over a hypersonic vehicle, with carbon vapor generated by surface ablation or by evaporation of amorphous carbon powder injected into the flow. Carbon atoms would then react with molecular oxygen present in the flow. To achieve optical gain sufficient for laser power generation, the rate of C atom production needs to be scaled up by at least an order of magnitude, compared to the yield obtained in the arc discharge used in the previous work. The approach used in the present work is to increase the high-temperature plasma volume, by using an inductively coupled, volumetric RF discharge sustained in a mixture of micron-size amorphous carbon particles and argon carrier gas, in a custom-design quartz cell. The temperature in the RF discharge, up to  $T = 2600$  K at the discharge power of 1 kW, is inferred from CO infrared emission spectra measured by a Fourier Transform Infrared (FTIR) spectrometer. Carbon vapor generated in the discharge is injected into the main low-temperature flow of argon or nitrogen, and

oxygen is added to the flow further downstream. Preliminary experiments indicate that at these conditions, vibrationally excited carbon monoxide, up to vibrational level  $v=6$ , is produced in the reaction of C atoms with oxygen molecules,  $C + O_2 \rightarrow CO(v) + O$ , at low-temperature conditions in the laser resonator,  $T = 400$  K. Vibrational level populations of the CO product generated by this reaction are inferred from CO infrared emission spectra. Further experiments quantifying the yield of vibrationally excited CO, as well as lasing tests, are underway.

## Acknowledgments

The experimental apparatus used in the present work was designed using the facilities of the Mechanical and Aerospace Engineering Department and fabricated to a high standard at the Chemical Physics glassblowing shop at the Ohio State University.

The CO synthetic spectrum code and the code for rotational temperature inference used to process the experimental data in this work have been generously shared by Elijah Jans.

The support of Lockheed Martin Corporation and project technical monitors Dr. Luke Uribarri and Dr. Ned Allen is gratefully acknowledged.

## Table of Contents

Abstract .....	iii
Acknowledgments .....	v
Table of Contents .....	vi
List of Figures .....	vii
Chapter 1. Introduction .....	10
1.1 Motivation .....	10
1.2 Previous Results .....	11
1.3 Objective .....	12
1.4 Approach .....	13
Chapter 2. Experimental .....	14
2.1 Overview of the Experimental Apparatus .....	14
2.2 ICP Discharge Cell .....	18
2.3 Carbon Powder Seeder .....	22
2.4 Temperature Measurements in the ICP Discharge .....	24
Chapter 3. Synthetic Spectrum Code .....	26
Chapter 4. Results and Discussion .....	27
4.1 Temperature in the ICP Discharge .....	27
4.2 CO Product Vibrational Populations .....	29
Chapter 5. Summary .....	33
Bibliography .....	35
Appendix A. Quartz ICP Cell #1 Engineering Drawings .....	36
Appendix B. Quartz ICP Cell #2 Engineering Drawings .....	39
Appendix C. Glass Observation Cell Engineering Drawing .....	42

## List of Figures

- Figure 1.1 Relative vibrational level populations of the CO product in the reaction between carbon vapor and molecular oxygen. Strong non-equilibrium distribution is achieved at both operating conditions. Absolute population inversion among levels  $v=4$  through  $v=7$  at the higher flow rate through the reactor of 12 SLM is apparent. Figure reproduced from (Jans, Frederickson and Yurkovich, et al. 2017). ..... 12
- Figure 2.1 Schematic of the experimental apparatus, including the gas delivery system and the electrical circuit. The carbon powder seeder, the ICP discharge cell, and the observation cell are connected in series. The carbon power carrier gas, the main flow, and the oxygen flow are supplied from gas cylinders through high-pressure regulators. The ICP discharge is powered by the high-voltage RF generator. The flow through the reactor is maintained by a high flow rate vacuum pump. The discharge coil and the ICP cell inlet are water cooled. Emission spectra are taken by an FTIR spectrometer. .... 16
- Figure 2.2 Schematic of the reactor operation. The carrier gas (Ar), seeded with carbon particles, is supplied to the ICP discharge cell and flows upward through the plasma in a swirling flow. The carbon vapor and the carrier gas are exhausted into the main flow channel and then into the observation cell. Oxygen is injected directly into the observation cell, where it is mixed with the carbon vapor. The reaction products flow along the observation cell towards exhaust to vacuum. .... 17
- Figure 2.3 Photograph of the experimental apparatus. The ICP discharge cell is placed on top of a ceramic insulation sheet and is supported by clamps mounted on acrylic plastic posts providing electrical insulation. The main flow channel is connected to the rest of the reactor by two 1" Swagelok Ultra-Torr fittings. The observation cell is supported by a clamp mounted on an acrylic post. The observation cell channels are attached to steel KF flanges by Agilent Torr Seal vacuum-ready epoxy. .... 18
- Figure 2.4 Schematic of the T-shaped ICP discharge cell. Argon carrier gas seeded with carbon particles enters the cell near the bottom through two inlet tubes fused tangentially to create a swirling flow in the discharge section. Carbon, evaporated inside the ICP plasma, is exhausted into the main flow through an orifice. The discharge coil, the quartz inlet tubes, and the metal supply lines are cooled by water. 21

Figure 2.5 Photographs of the ICP plasma. Left: plasma sustained in a 19.3 Torr total pressure, 0.5 SLM flow of argon, at RF power of 1400 W. Right: plasma sustained in XX Torr total pressure, X.X SLM flow of argon seeded with carbon particles. Blue glow (C <sub>2</sub> Swan bands indicates presence of C and C <sub>2</sub> in the discharge section.....	21
Figure 2.6 Photo of the older version ICP discharge cell in operation. The extension of the plasma into the argon buffer flow in the main channel and into the observation cell, all the way to the vacuum exhaust port, is clearly visible. Replacing argon in the buffer flow with nitrogen helps confining the plasma within the ICP discharge cell, as shown in Figure 2.5.....	22
Figure 2.7 Schematic of the carbon powder seeder, including gas delivery system. Carbon powder is stored in the acrylic plastic container at the bottom. A metal flange with two feedthroughs is vacuum-sealed to the container using a rubber O-ring. The carrier gas flows through the container, entraining carbon powder. A bypass line is also available. An evacuation line is added to reduce the pressure inside the seeder container before connecting it to the main flow.....	23
Figure 2.8 Photograph of the carbon particle seeder supplied by the Lockheed Martin Co. Left: full assembly; right: the container filled with the carbon powder during operation.....	24
Figure 2.9 Schematic of an auxiliary apparatus used for temperature measurements in the ICP discharge. The discharge is sustained in a horizontal glass cell. A mixture of argon and carbon monoxide supplied from gas cylinders flows through the discharge and exhausts into vacuum. Then FTIR spectrometer with a focusing mirror arrangement is used to collect CO emission spectra from the plasma. ....	25
Figure 2.10 Photograph of the ICP discharge sustained in Ar-CO flow. Coupled RF power 1000 W, total pressure 20 Torr, 2.5% of CO in Ar, flow rate through the cell 0.5 SLM. ....	25
Figure 4.1 Part of the CO fundamental emission spectrum in the ICP discharge. Coupled RF power 1000 W, total pressure 20 Torr, 2.5% of CO in Ar, flow rate through the cell 0.5 SLM. ....	28
Figure 4.2 Boltzmann plot of R-branch of the CO( $v=1 \rightarrow 0$ ) vibrational band emission from the ICP discharge cell. Coupled RF power 1000 W, total pressure 20 Torr, 2.5% of CO in Ar, flow rate through the cell 0.5 SLM. Best fit rotational-translational temperature is $T=2700 \pm 40$ K. ....	28
Figure 4.3 Temperature in the ICP discharge inferred from CO fundamental emission spectra such as shown in Figure 4.2, plotted vs. RF discharge power. For all measurements, total pressure 20 Torr, 2.5% of CO in Ar, flow rate through the cell 0.5 SLM. ....	29



Figure 4.4 CO product fundamental emission spectrum from observation cell. Coupled RF power 1400 W, discharge sustained in a carbon-seeded flow of Ar, at total pressure of 19.3 Torr and 0.5 SLM flow rate. Main flow rate 5 SLM, oxygen added at 7 Torr partial pressure. ....	30
Figure 4.5 Comparison of the CO product fundamental emission spectrum and best fit synthetic spectrum used for the CO vibrational population inference. Top: full spectrum in the range of interest. Bottom: enlarged view of a portion of the spectrum. Coupled RF power 1400 W, discharge sustained in a carbon-seeded flow of Ar, at total pressure of 19.3 Torr and 0.5 SLM flow rate. Main flow rate 5 SLM, oxygen added at 7 Torr partial pressure.....	31
Figure 4.6 Boltzmann plot of the R-branch of CO( $v=1 \rightarrow 0$ ) vibrational band emission in the observation cell. Coupled RF power 1400 W, discharge sustained in a carbon-seeded flow of Ar, at total pressure of 19.3 Torr and 0.5 SLM flow rate. Main flow rate 5 SLM, oxygen added at 7 Torr partial pressure. Best fit rotational-translational temperature is $T=400 \pm 10$ K. ....	32
Figure 4.7 Normalized relative vibrational populations of CO product, inferred from the synthetic spectrum plotted in Figure 4.5. Coupled RF power 1400 W, discharge sustained in a carbon-seeded flow of Ar, at total pressure of 19.3 Torr and 0.5 SLM flow rate. Main flow rate 5 SLM, oxygen added at 7 Torr partial pressure.....	32

## Chapter 1. Introduction

### 1.1 Motivation

Exothermic chemical reactions are widely used for extraction of useful work from the chemical energy of fuels, by chemically converting the precursors to lower-energy species and utilizing the excess chemical energy, i.e. the reaction enthalpy. In chemical lasers, this excess energy is stored in the internal modes of the reaction products and is released by a process of stimulated emission, in the form of a beam of collimated coherent light. It has been predicted that in the exothermic reaction between carbon atoms and molecular oxygen, nearly 30% of the reaction enthalpy can be stored in the vibrational modes of the carbon monoxide product (Schatz 2013), which indicates the feasibility of development of a new kind of chemical carbon monoxide (CO) laser.

An application of such laser could be to generate electrical power for the on-board electronics of a future hypersonic vehicle that uses a supersonic ramjet (scramjet) type engine for propulsion. In such engines, air is compressed not by a rotating mechanical compressor, but by the forward motion of the vehicle through the atmosphere. In scramjet engines, a conventional turbine / electrical generator cannot be used to convert the chemical energy of the jet fuel into electrical power, due to high losses caused by shock wave formation. Batteries, on the other hand, have low energy density and would considerably

limit the range of the light, compact unmanned hypersonic vehicle. The new CO laser would use the energy of the high-speed airflow to heat and sublime solid amorphous carbon carried on board as a chemical fuel, to generate carbon vapor, which would produce strongly vibrationally excited carbon monoxide by a chemical reaction with the molecular oxygen present in the airflow and create population inversion during subsequent supersonic expansion, enabling laser action. The conversion to laser output power electrical power could be completed using photovoltaic cells.

## 1.2 Previous Results

Vibrational level populations of the CO product in the reaction  $C + O_2 \rightarrow CO(v>0) + O$  were measured in a previous experiment conducted at the Non-Equilibrium Thermodynamics Laboratories (NETL). In the experiment, carbon vapor produced by heating two graphite electrodes by a high-current arc discharge was entrained by a buffer flow of argon and mixed with oxygen injected downstream of the arc discharge cell. The emission spectrum of the CO reaction product was obtained in situ, using a Fourier-transform Infrared (FTIR) detector. It was shown that the CO product is strongly vibrationally excited, with absolute population inversions among levels  $v=4$  through  $v=7$ , as shown in Figure 1.1 (Jans, Frederickson and Yurkovich, et al. 2017). Nevertheless, sustained lasing has not been achieved in this study, most likely due to low yield of the vibrationally excited CO product.

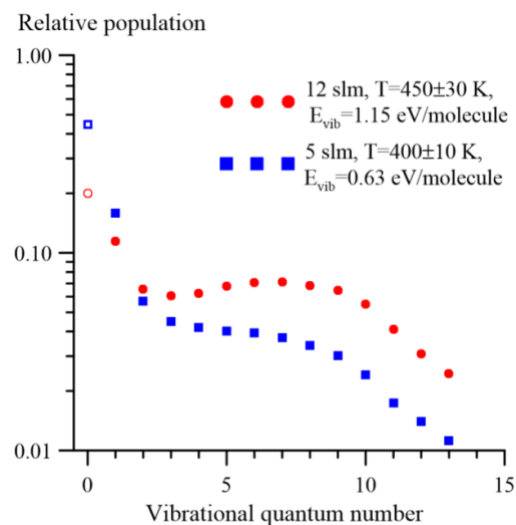


*Figure 1.1 Relative vibrational level populations of the CO product in the reaction between carbon vapor and molecular oxygen. Strong non-equilibrium distribution is achieved at both operating conditions. Absolute population inversion among levels  $v=4$  through  $v=7$  at the higher flow rate through the reactor of 12 SLM is apparent. Figure reproduced from (Jans, Frederickson and Yurkovich, et al. 2017).*

### 1.3 Objective

In order to make this approach feasible for the development of the new chemical CO laser, the yield of vibrationally excited carbon monoxide needs to be scaled up considerably, by up to several orders of magnitude. This estimate is based on a previous study of an optically pumped CO laser (Ivanov, et al. 2013) and is backed by measurements of the fraction of atomic carbon in the arc discharge products using a Residual Gas Analyzer (Jans, Frederickson and Gulko, et al. 2018).

## 1.4 Approach

Since molecular oxygen is stable and readily available, the yield of carbon monoxide is limited only by the amount of atomic carbon vapor supplied to the reaction region. To scale up the generation of carbon vapor, in the present work the arc discharge is replaced with a volumetric Inductively Coupled Plasma (ICP) generated by a 13.56 MHz RF voltage. The ICP has the potential of increasing the volume of high-temperature plasma from a few mm<sup>3</sup> to several tens of cm<sup>3</sup>. Carbon is supplied into the ICP discharge in the form of a fine powder (1-5-μm-size amorphous carbon particles), which dramatically increases the surface area and enhances surface heating of the carbon particles in the plasma.

## Chapter 2. Experimental

### 2.1 Overview of the Experimental Apparatus

The experimental setup consists of a custom-designed carbon particle seeder provided by Lockheed Martin Co., a new custom-made quartz ICP discharge cell, and an observation cell made of glass, arranged as shown in Figure 2.1 and Figure 2.2. A continuous flow through the system is established using a UNI-VAC uv400 high-flow rate vacuum pump. The buffer gas (Ar, N<sub>2</sub>, or dry air) is supplied from a high-pressure gas cylinder into the main flow channel. The carbon particle carrier gas (Ar), from another gas cylinder flows through the carbon powder seeder, where it entrains the carbon particles into the ICP discharge cell exhausting into the main flow channel. Thus, the flow heated in the ICP discharge, containing the carbon particles and carbon vapor is injected into the main buffer flow through an orifice 5 to 7 mm in diameter, and is delivered to the observation cell, where oxygen is added to the flow, initiating a chemical reaction with carbon vapor. The reaction products flow through the observation cell and are exhausted to vacuum. Emission spectra from the flow in the observation cell are obtained using a Varian 660-IR FTIR spectrometer operated in emission mode. Emission from the flow is focused into emission port of the spectrometer, using off-axis parabolic mirrors.

The ICP discharge is sustained using a 10.5-turn copper coil powered by a Dressler 13.56 MHz, 5 kW Radio Frequency (RF) generator and an automatic impedance matching box. A heavy-duty 25-pF capacitor is connected in series with the coil, to improve impedance matching. In all present experiments, the RF power reflected back (i.e. not coupled to the plasma) did not exceed a few tens of Watts. However, impedance matching could not be achieved without using an additional stray capacitor (an insulated piece of wire ~50 cm long connected to the high-voltage side of the heavy-duty capacitor).

Infrared emission from the flow is taken through calcium fluoride ( $\text{CaF}_2$ ) optical access windows, which transmit over 90% of emission in the near- and mid- infrared regions (for wavelengths up to 8  $\mu\text{m}$  or wavenumbers down to 1250  $\text{cm}^{-1}$ ). Argon purge lines were added to the observation cell, to prevent accumulation of carbon powder in the flow recirculation regions near the optical access windows, as shown in Figure 2.1. Both the ICP discharge cell and the observation cell are enclosed in a Faraday cage made of copper mesh, to shield the FTIR spectrometer from the electromagnetic interference produced by the discharge.

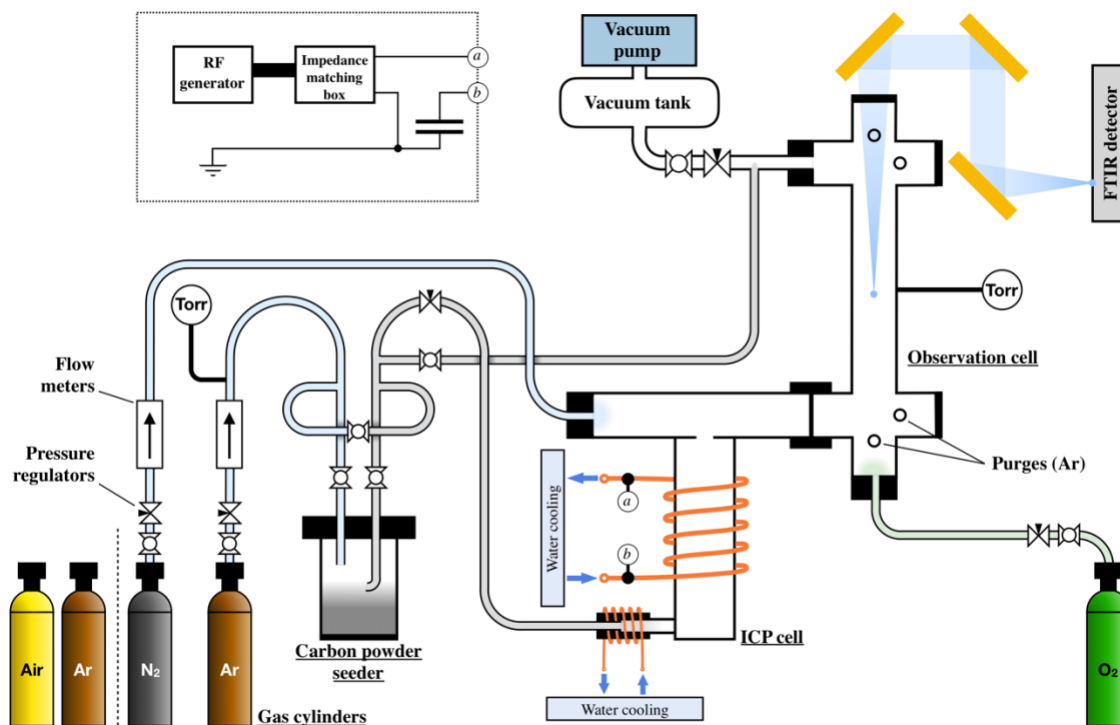
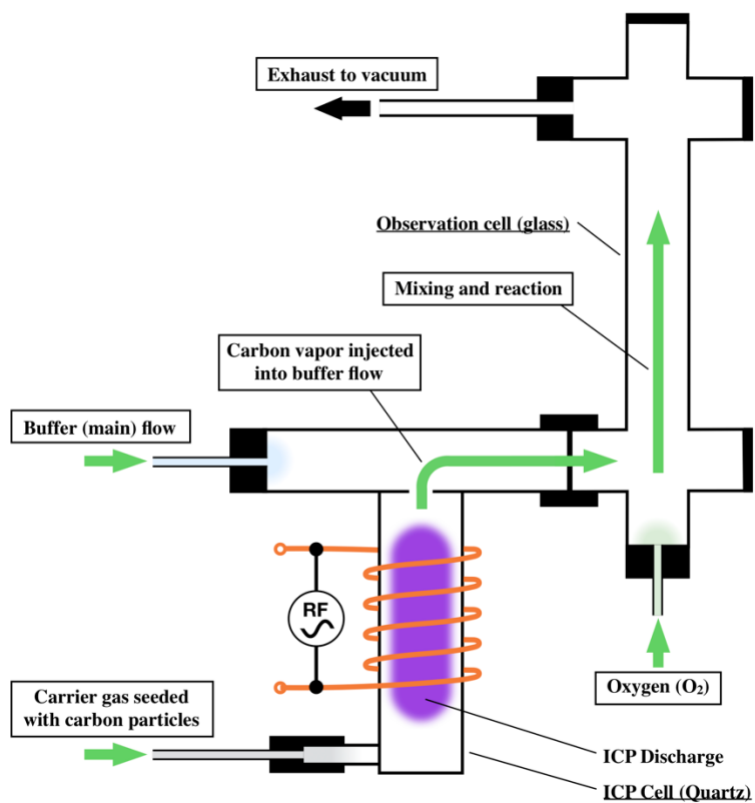
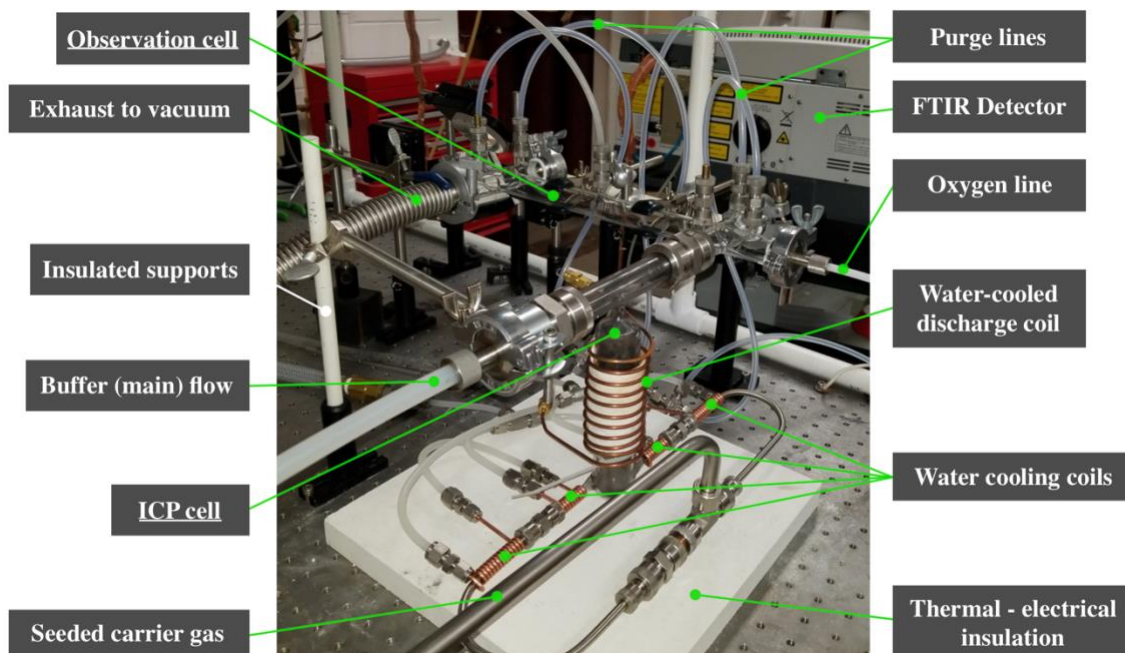


Figure 2.1 Schematic of the experimental apparatus, including the gas delivery system and the electrical circuit. The carbon powder seeder, the ICP discharge cell, and the observation cell are connected in series. The carbon power carrier gas, the main flow, and the oxygen flow are supplied from gas cylinders through high-pressure regulators. The ICP discharge is powered by the high-voltage RF generator. The flow through the reactor is maintained by a high flow rate vacuum pump. The discharge coil and the ICP cell inlet are water cooled. Emission spectra are taken by an FTIR spectrometer.





*Figure 2.2 Schematic of the reactor operation. The carrier gas (Ar), seeded with carbon particles, is supplied to the ICP discharge cell and flows upward through the plasma in a swirling flow. The carbon vapor and the carrier gas are exhausted into the main flow channel and then into the observation cell. Oxygen is injected directly into the observation cell, where it is mixed with the carbon vapor. The reaction products flow along the observation cell towards exhaust to vacuum.*



*Figure 2.3 Photograph of the experimental apparatus. The ICP discharge cell is placed on top of a ceramic insulation sheet and is supported by clamps mounted on acrylic plastic posts providing electrical insulation. The main flow channel is connected to the rest of the reactor by two 1" Swagelok Ultra-Torr fittings. The observation cell is supported by a clamp mounted on an acrylic post. The observation cell channels are attached to steel KF flanges by Agilent Torr Seal vacuum-ready epoxy.*

## 2.2 ICP Discharge Cell

The T-shaped ICP discharge cell has a vertical cylindrical discharge section, 1.5 inch in diameter and 5¾-inch long, and a horizontal 1-inch diameter channel for the main buffer flow, as shown in Figure 2.4. The carrier gas seeded with carbon particles enters the cell at the bottom of the discharge section through two ¼ inch diameter tubes fused to the cell tangentially, to generate a swirling flow through the plasma. The discharge products are exhausted into the main flow channel through a 5-mm diameter orifice. The second ICP discharge cell used in the present work has a similar configuration, except that the

discharge section is 6½ inches long, the inlet tubes are ½ inch in diameter, and the exhaust orifice is 7-mm diameter.

As discussed in Chapter 4, the temperature in the ICP discharge is very high (up to  $T \approx 2700$  K at 1000 W of RF power coupled). To avoid the cell damage at such high temperatures, the entire cell is made of quartz, which has a melting point of approximately 2000 K. Originally, the ICP discharge cell was not designed to be cooled. However, at RF discharge power above ~1000 W and run times of around 30 seconds, the cell temperature became so high that the rubber O-rings in the Swagelok Ultra-Torr fittings conjoining the carrier gas line to the quartz inlet tubes were burnt. Also, the copper induction coil showed severe signs of overheating, approaching melting point. To enable continuous operation at higher RF discharge power, (a) the induction coil was made of 1/8-inch-diameter copper tubing and water cooled, (b) additional water-cooling coils, also made of 1/8-inch copper tubing, were placed around the quartz discharge cell inlet tubes and the metal carrier gas delivery lines, as shown in Figure 2.3 and Figure 2.4, to keep the temperature around the O-rings low. Using this approach prevented the overheating of the induction coil and the ICP discharge cell and allowed operation at RF discharge power of up to 2000 W and runtime of up to at least a minute.

At normal operating conditions, the plasma sustained in the discharge section is diffuse and fills the entire cell volume, as shown in Figure 2.5. In argon flow without carbon particles, the plasma appears purple, as seen in the left figure. When carbon particles

are added to the argon flow, blue emission is detected from the plasma, most likely due to C<sub>2</sub> Swan emission bands, indicating C atom and C<sub>2</sub> radical formation in the discharge.

It was observed that at high RF discharge power, the ICP plasma emission extends far into the main Ar flow, extending all the way into the observation cell, as shown in Figure 2.6. This extension of the plasma into the mixing and reaction region of the observation cell presents a problem, since vibrationally excited CO may be formed in plasma chemical reactions, e.g. by electron impact excitation, instead of a “conventional” exothermic chemical reaction between C atoms and O<sub>2</sub> molecules. To contain the plasma within the ICP discharge cell, argon in the buffer flow was replaced with nitrogen. This change resulted in a remarkable improvement in the containment of the ICP plasma, keeping it mostly within the discharge section.

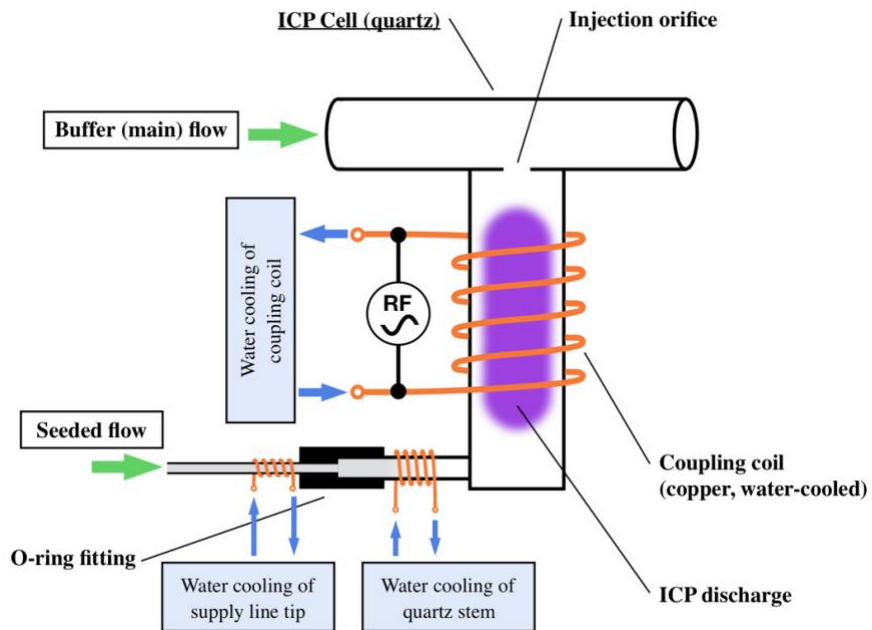


Figure 2.4 Schematic of the T-shaped ICP discharge cell. Argon carrier gas seeded with carbon particles enters the cell near the bottom through two inlet tubes fused tangentially to create a swirling flow in the discharge section. Carbon, evaporated inside the ICP plasma, is exhausted into the main flow through an orifice. The discharge coil, the quartz inlet tubes, and the metal supply lines are cooled by water.

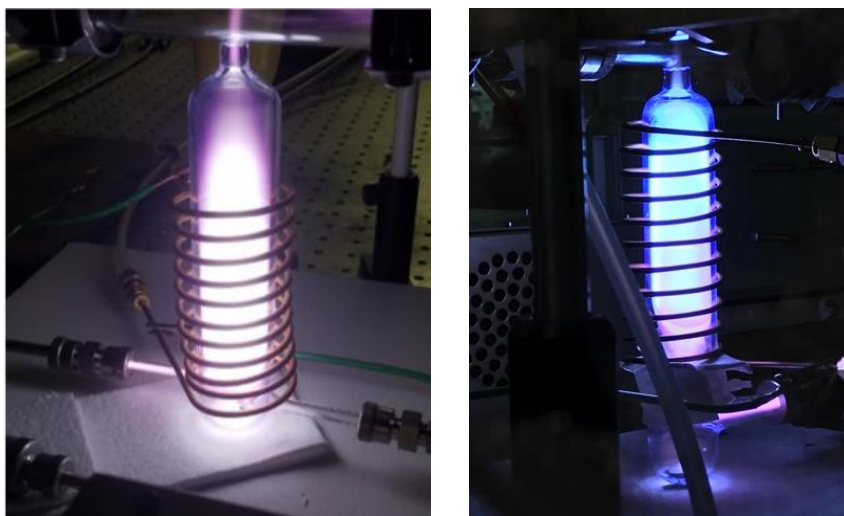
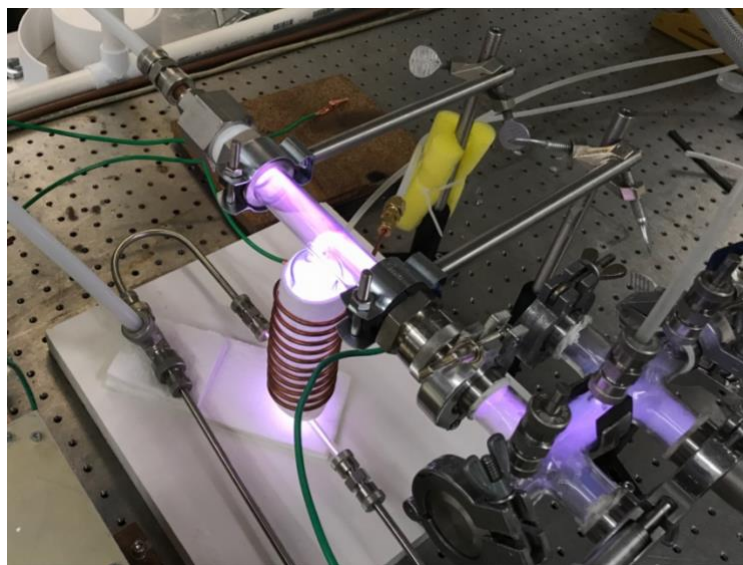


Figure 2.5 Photographs of the ICP plasma. Left: plasma sustained in a 19.3 Torr total pressure, 0.5 SLM flow of argon, at RF power of 1400 W. Right: plasma sustained in 6 Torr total pressure flow of argon seeded with carbon particles. Blue glow ( $C_2$  Swan bands indicates presence of C and  $C_2$  in the discharge section).



*Figure 2.6 Photo of the older version ICP discharge cell in operation. The extension of the plasma into the argon buffer flow in the main channel and into the observation cell, all the way to the vacuum exhaust port, is clearly visible. Replacing argon in the buffer flow with nitrogen helps confining the plasma within the ICP discharge cell, as shown in Figure 2.5.*

### **2.3 Carbon Powder Seeder**

The micron-sized carbon particles are added to the carrier Ar gas flow using a custom-made seeder provided by Lockheed Martin Co. The carbon powder is stored inside an acrylic plastic container, vacuum-sealed using a rubber O-ring to a metal flange with two feedthroughs, as shown in Figure 2.7. The carrier gas flow through the container entrains the carbon particles. The flow in and out of the container is controlled by two ball valves, and a bypass line is available if operation without the carbon particles is needed.

During the experiment, the gas delivery system was modified to include an additional evacuation line used to reduce the pressure in the carbon powder container before connecting it to the main flow. This was done to avoid adding a large amount of

carbon powder to the flow in the beginning of the run, due to significant initial pressure difference. The experimental procedure includes adjusting the argon carrier flow through the seeder, with the needle valve on the seeder exit line closed, and the evacuation line valve open, and then gradually opening the valve on the exit line while at the same time shutting down the evacuation line valve (refer to schematic in Figure 2.7).

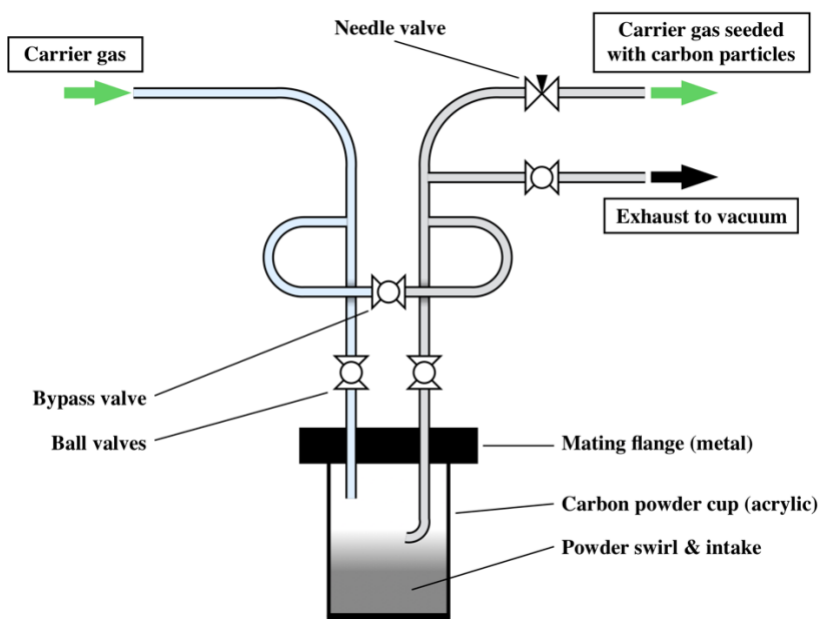


*Figure 2.7 Schematic of the carbon powder seeder, including gas delivery system. Carbon powder is stored in the acrylic plastic container at the bottom. A metal flange with two feedthroughs is vacuum-sealed to the container using a rubber O-ring. The carrier gas flows through the container, entraining carbon powder. A bypass line is also available. An evacuation line is added to reduce the pressure inside the seeder container before connecting it to the main flow.*

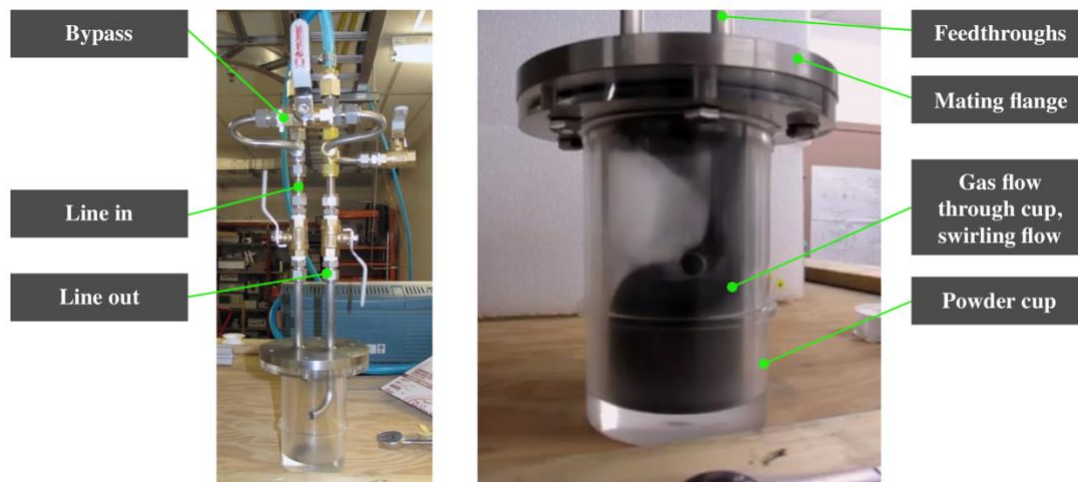


*Figure 2.8 Photograph of the carbon particle seeder supplied by the Lockheed Martin Co. Left: full assembly; right: the container filled with the carbon powder during operation.*

## 2.4 Temperature Measurements in the ICP Discharge

An auxiliary separate experimental apparatus, illustrated in Figure 2.9, is used for temperature measurements in the ICP discharge plasma. For this, the discharge is sustained inside of a horizontal cylindrical glass cell 2.5 inches in diameter, in an argon flow seeded with 2.5% CO at a total pressure of 20 Torr and a 0.5 SLM flow rate. The plasma generated at these conditions is diffuse and fills the entire volume of the cell, as shown in Figure 2.10. The use of Agilent Torr-Seal epoxy to attach the glass cell to metal KF flanges limited the maximum discharge power due to overheating, such that during these measurements the discharge power could not exceed 1000 W, and the run time was kept short, in the range of several seconds. The discharge cell is enclosed in a Faraday cage made of copper mesh, to shield the FTIR spectrometer from the electromagnetic interference produced by the discharge. Optical access for acquiring infrared emission spectra is provided by a  $\text{CaF}_2$  window at one end of the discharge cell.



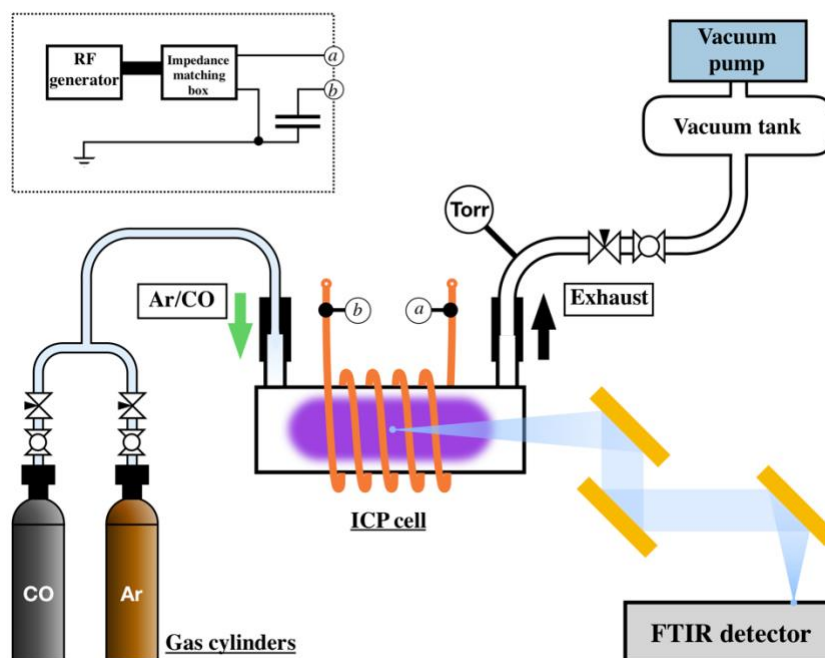


Figure 2.9 Schematic of an auxiliary apparatus used for temperature measurements in the ICP discharge. The discharge is sustained in a horizontal glass cell. A mixture of argon and carbon monoxide supplied from gas cylinders flows through the discharge and exhausts into vacuum. Then FTIR spectrometer with a focusing mirror arrangement is used to collect CO emission spectra from the plasma.



Figure 2.10 Photograph of the ICP discharge sustained in Ar-CO flow. Coupled RF power 1000 W, total pressure 20 Torr, 2.5% of CO in Ar, flow rate through the cell 0.5 SLM.

### Chapter 3. Synthetic Spectrum Code

Relative populations of vibrational-rotational levels of the CO product, and of CO added to the flow for temperature measurements in the ICP discharge, are inferred from CO infrared emission spectra taken in the observation cell, as shown in Figure 2.1. For this, a synthetic spectrum code is used (Jans, Frederickson and Yurkovich, et al. 2017). Briefly, the code generates a synthetic emission spectrum of CO and determines CO vibrational level populations (for vibrational quantum number  $v>0$ ) that provide best match to the experimental spectrum. The code incorporates accurate Einstein coefficients for CO spontaneous emission (from fundamental to third overtone) and the FTIR spectrometer instrument function (apparent spectral line width), which controls the resolution of the experimental spectrum. The rotational-translational temperature, used as one of the code inputs, is determined from the slope of the Boltzmann plot for rotational populations of the fundamental emission band  $v=1\rightarrow 0$ .

The population of the ground CO vibrational level,  $v=0$ , is obtained by extrapolating the CO vibrational distribution for  $v>0$  to  $v=0$  in the semi-log scale. Finally, the vibrational populations inferred using the synthetic spectrum code and the  $v=0$  population are normalized to yield relative populations (see Figure 4.7).

## Chapter 4. Results and Discussion

### 4.1 Temperature in the ICP Discharge

To assess the feasibility of vaporizing carbon using an ICP discharge, the temperature in the plasma was measured using the setup discussed in Section 2.4 (see Figure 2.9 and Figure 2.10). The ICP discharge is sustained in a flow of argon seeded with 2.5 % of CO, at total pressure 20 Torr, flow rate 0.5 SLM, and RF discharge power of up to 1000 W. The emission spectrum shown in Figure 2.1 is obtained from approximately the center of the discharge, and the temperature was found from the slope of the best linear fit to the R-branch of the CO fundamental emission band spectrum on a Boltzmann plot, as shown in Figure 4.2. The temperature inferred in this way is plotted for discharge powers ranging from 100 W to 1000W in Figure 4.3. The error bars in Figure 4.3 represent the uncertainty of the linear fit. At the highest coupled power of 1000 W, the temperature in the discharge is  $T = 2700 \pm 44$  K. While this temperature is lower than the sublimation point of amorphous carbon,  $T = 3900$  K, it is expected that the temperature in the ICP discharge cell in the main experimental apparatus, discussed in Section 2.1, would be higher, since operation at higher discharge powers and longer run times are possible.

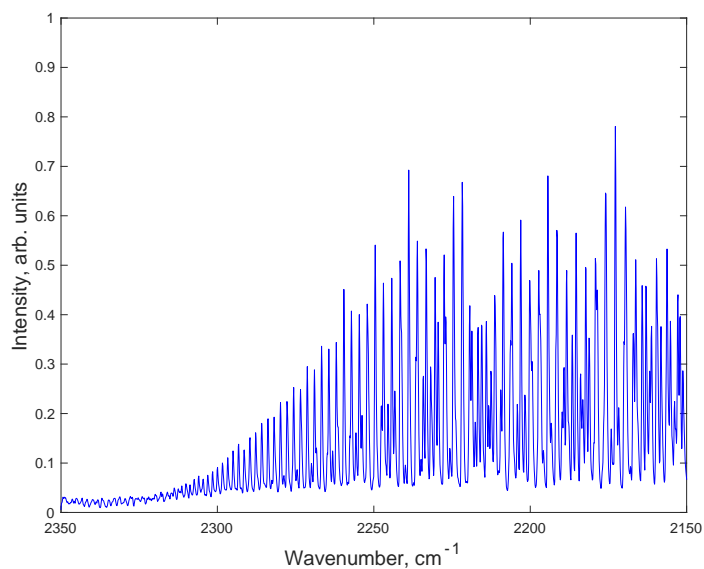


Figure 4.1 Part of the CO fundamental emission spectrum in the ICP discharge. Coupled RF power 1000 W, total pressure 20 Torr, 2.5% of CO in Ar, flow rate through the cell 0.5 SLM.

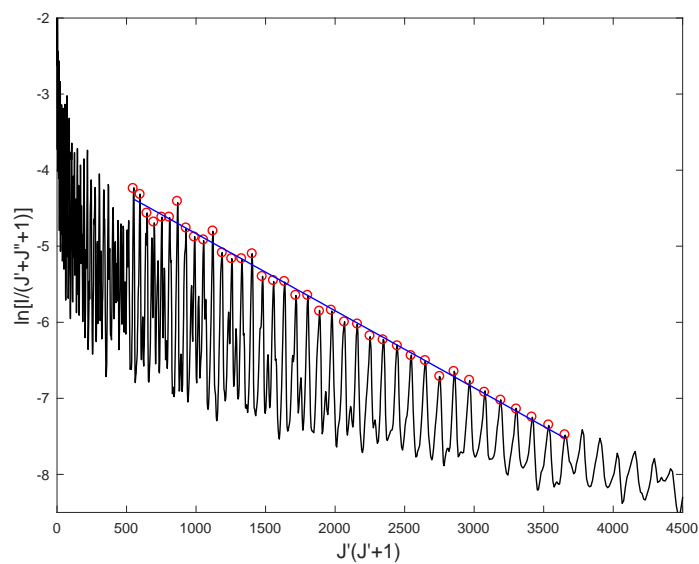
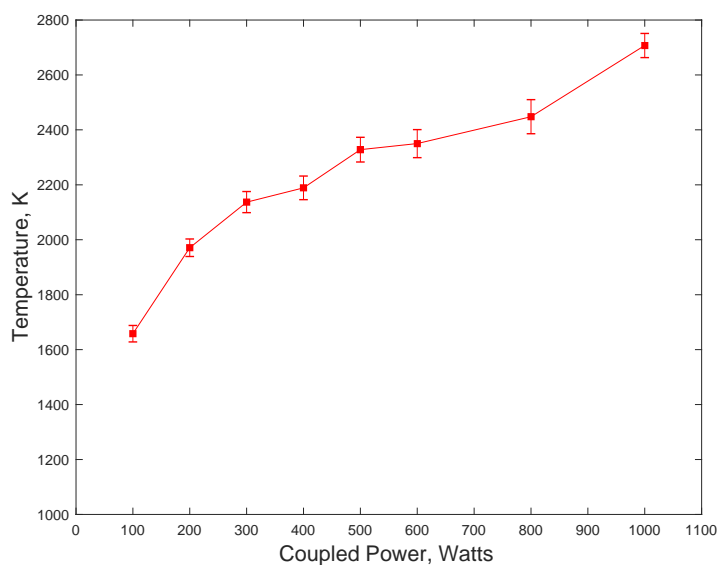


Figure 4.2 Boltzmann plot of R-branch of the CO( $v=1 \rightarrow 0$ ) vibrational band emission from the ICP discharge cell. Coupled RF power 1000 W, total pressure 20 Torr, 2.5% of CO in Ar, flow rate through the cell 0.5 SLM. Best fit rotational-translational temperature is  $T=2700 \pm 40$  K.



*Figure 4.3 Temperature in the ICP discharge inferred from CO fundamental emission spectra such as shown in Figure 4.2, plotted vs. RF discharge power. For all measurements, total pressure 20 Torr, 2.5% of CO in Ar, flow rate through the cell 0.5 SLM.*

## 4.2 CO Product Vibrational Populations

The vibrational populations of the CO produced by the chemical reaction between carbon vapor generated in the ICP discharge and molecular oxygen were measured using the experimental apparatus discussed in Section 2.1. The discharge is sustained in a flow of argon seeded with carbon particles, at a total pressure of 19.3 Torr and a flow rate of 0.5 SLM, with a coupled power of 1400 W. The flow from the discharge cell is exhausted into a 5 SLM main buffer flow of argon and enters the observation cell, where molecular oxygen is injected at a partial pressure of 7 Torr. The emission spectrum shown in Figure 4.4, obtained near the center of the observation cell, indicates the presence of vibrationally excited CO. Using the synthetic spectrum code discussed in Chapter 3, a best fit synthetic spectrum is generated, and the populations of the CO product vibrational

levels are inferred. Figure 4.5 illustrates good agreement between the experimental and the synthetic spectra. The rotational-translational temperature inferred from the rotational structure of the CO fundamental emission band as shown in Figure 4.6, is much lower than the temperature in the ICP discharge cell,  $T = 400\text{K}$ , due to strong dilution of the flow exiting the discharge cell by the main buffer flow. Figure 4.7, which plots CO vibrational level populations inferred from the synthetic spectra, shows that the CO product is vibrationally excited, and vibrational levels up to level  $v=6$  are detected. It can be seen that the CO vibrational distribution is non-Boltzmann, with the vibrational temperature (obtained from the slope of the distribution) of  $T_v \approx 2900\text{ K}$  for  $v=0,1,2$ . Vibrational levels  $v=3-6$  have higher populations, indicating that partial population inversion among the vibrational-rotational levels of the CO product may be possible.

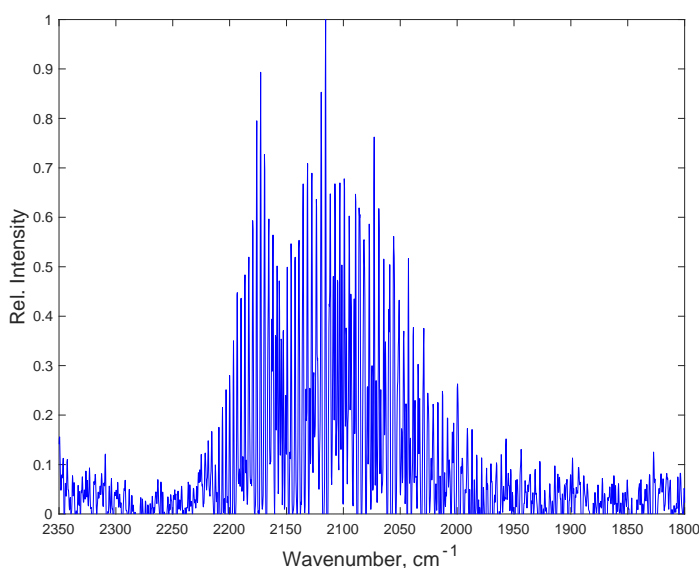


*Figure 4.4 CO product fundamental emission spectrum from observation cell. Coupled RF power 1400 W, discharge sustained in a carbon-seeded flow of Ar, at total pressure of 19.3 Torr and 0.5 SLM flow rate. Main flow rate 5 SLM, oxygen added at 7 Torr partial pressure.*

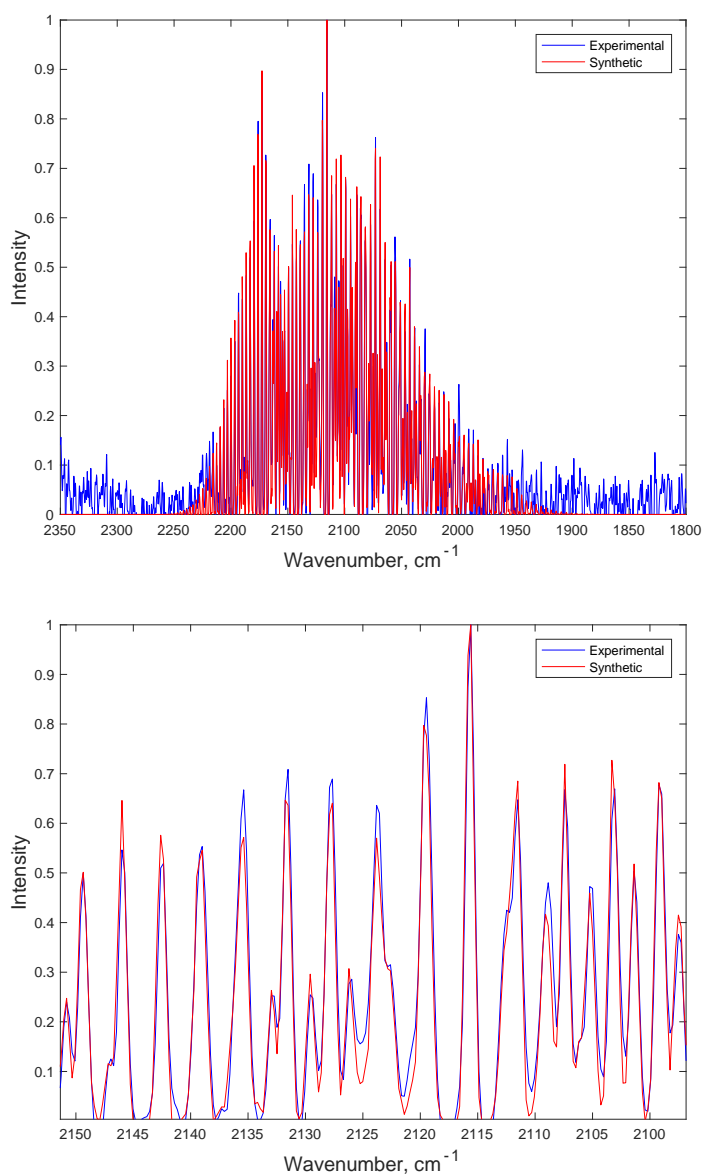


*Figure 4.5 Comparison of the CO product fundamental emission spectrum and best fit synthetic spectrum used for the CO vibrational population inference. Top: full spectrum in the range of interest. Bottom: enlarged view of a portion of the spectrum. Coupled RF power 1400 W, discharge sustained in a carbon-seeded flow of Ar, at total pressure of 19.3 Torr and 0.5 SLM flow rate. Main flow rate 5 SLM, oxygen added at 7 Torr partial pressure.*

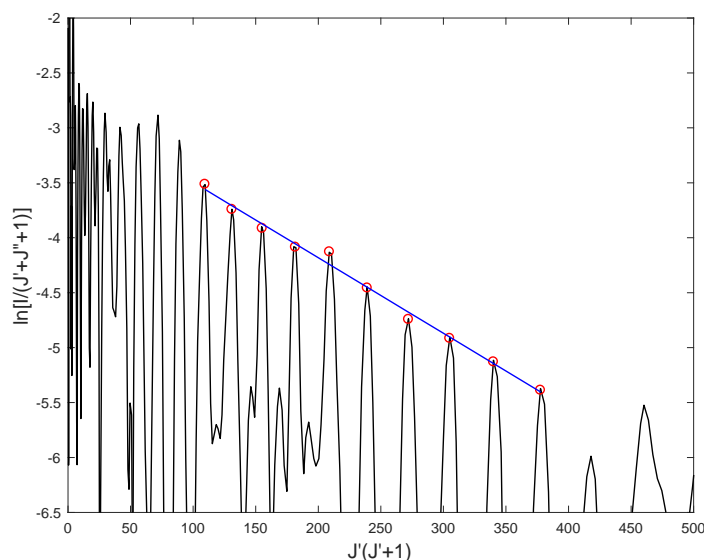


Figure 4.6 Boltzmann plot of the R-branch of  $\text{CO}(v=1 \rightarrow 0)$  vibrational band emission in the observation cell. Coupled RF power 1400 W, discharge sustained in a carbon-seeded flow of Ar, at total pressure of 19.3 Torr and 0.5 SLM flow rate. Main flow rate 5 SLM, oxygen added at 7 Torr partial pressure. Best fit rotational-translational temperature is  $T=400 \pm 10$  K.

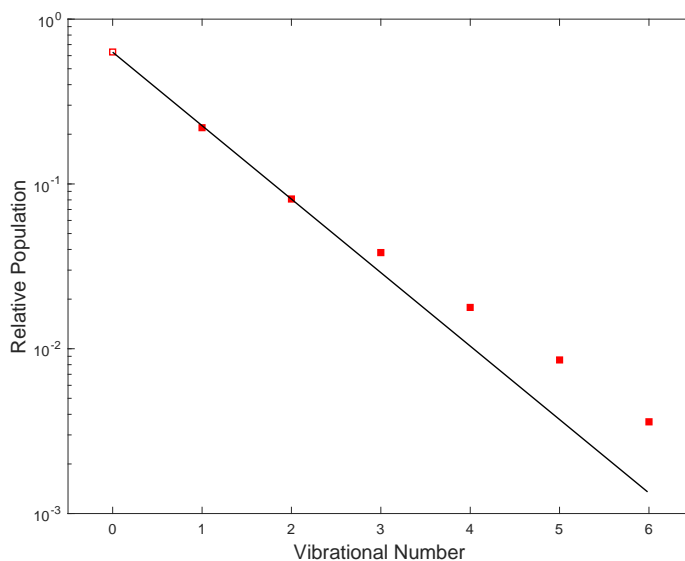


Figure 4.7 Normalized relative vibrational populations of CO product, inferred from the synthetic spectrum plotted in Figure 4.5. Coupled RF power 1400 W, discharge sustained in a carbon-seeded flow of Ar, at total pressure of 19.3 Torr and 0.5 SLM flow rate. Main flow rate 5 SLM, oxygen added at 7 Torr partial pressure.



## Chapter 5. Summary

In this work, a new experimental apparatus using a volumetric Inductively Coupled Plasma (ICP) RF discharge is designed, assembled, and tested. The ICP discharge is used to generate vapor-phase carbon for the chemical reaction with molecular oxygen  $O_2$ , producing vibrationally excited carbon monoxide (CO) product. Feasibility of using the ICP plasma for high-yield vaporization of amorphous carbon is assessed using an auxiliary apparatus, where the ICP discharge is sustained in a 20 Torr, 5 SLM flow of argon seeded with 2.5 % of CO, used as a thermometric element. The temperature inside the ICP plasma inferred from the rotational structure of the fundamental band ( $v=1 \rightarrow 0$ ) of the CO emission spectrum is  $T = 2700 \pm 44$  K at the coupled RF power of 1000 W. Although this temperature is lower than the sublimation point of amorphous carbon,  $T = 3900$  K, it is expected that the temperature in the ICP discharge cell in the main experimental apparatus, operated at higher RF discharge power and longer run time, would be significantly higher.

In the experiment where the ICP discharge is sustained at a coupled RF power of 1400 W in a flow of argon seeded with micron-sized amorphous carbon particles, at 19.3 Torr and 0.5 SLM, with oxygen added downstream of the discharge, vibrationally excited CO reaction product is detected from FTIR emission spectra. Relative populations of the

CO product vibrational levels are inferred from the emission spectra, and excitation up to vibrational level  $v=6$  is observed. The CO vibrational distribution is non-Boltzmann, with the vibrational temperature of  $T_v \approx 2900$  K among levels  $v=0-2$ . Vibrational levels  $v=3-6$  have higher populations. Rotational-translational temperature in the flow at these conditions is relatively low,  $T = 400$  K. These results indicate that a partial population inversion among the rotational levels of the CO product may be obtained in the observation cell, creating conditions where lasing action is possible.

Future work will be directed towards increasing the yield of carbon vapor generated in the ICP discharge, evaluated from calibrated FTIR absorption spectra of CO product, to generate a sufficient amount of excited CO product in the observation cell for lasing action. In a lasing test, an optical resonator will be set up, using partially transmitting mirrors positioned at the two ends of the observation cell. Vibrationally excited CO will act as the gain medium, with a continuous supply of the excited CO product generated by the chemical reaction between carbon vapor and molecular oxygen. If the process of stimulated emission in the resonator is self-sustained, the experimental apparatus developed in the present work would be the first working prototype of a new chemical CO laser operating at steady-state conditions.

## Bibliography

- Ivanov, E., K. Frederickson, S. Leonov, Lempert W.R., Adamovich I.V., and Rich J.W. 2013. "Optically Pumped Carbon Monoxide Laser Operating at Elevated Temperatures." *Laser Physics* 23: 095004.
- Jans, E., K. Frederickson, I. Gulko, J.W. Rich, and I.V. Adamovich. 2018. "Scaling Up Generation of Vibrationally Excited CO in a Chemical Reaction between Carbon Vapor and Oxygen." Kissimmee, FL: AIAA Paper 2018-0179, 56th AIAA Aerospace Sciences Meeting (SciTech 2018), 8-12 January.
- Jans, E., K. Frederickson, M. Yurkovich, J.W. Rich, and I.V. Adamovich. 2017. "Progress in Development of a Chemical CO Laser Driven by a Chemical Reaction between Carbon Vapor and Oxygen." Grapevine, TX: AIAA Paper 2017-1967, 55th AIAA Aerospace Sciences Meeting (SciTech 2017), 9-13 January.
- Schatz, G. 2013. Department of Chemistry, Northwestern University, Private Communication.

## Appendix A. Quartz ICP Cell #1 Engineering Drawings

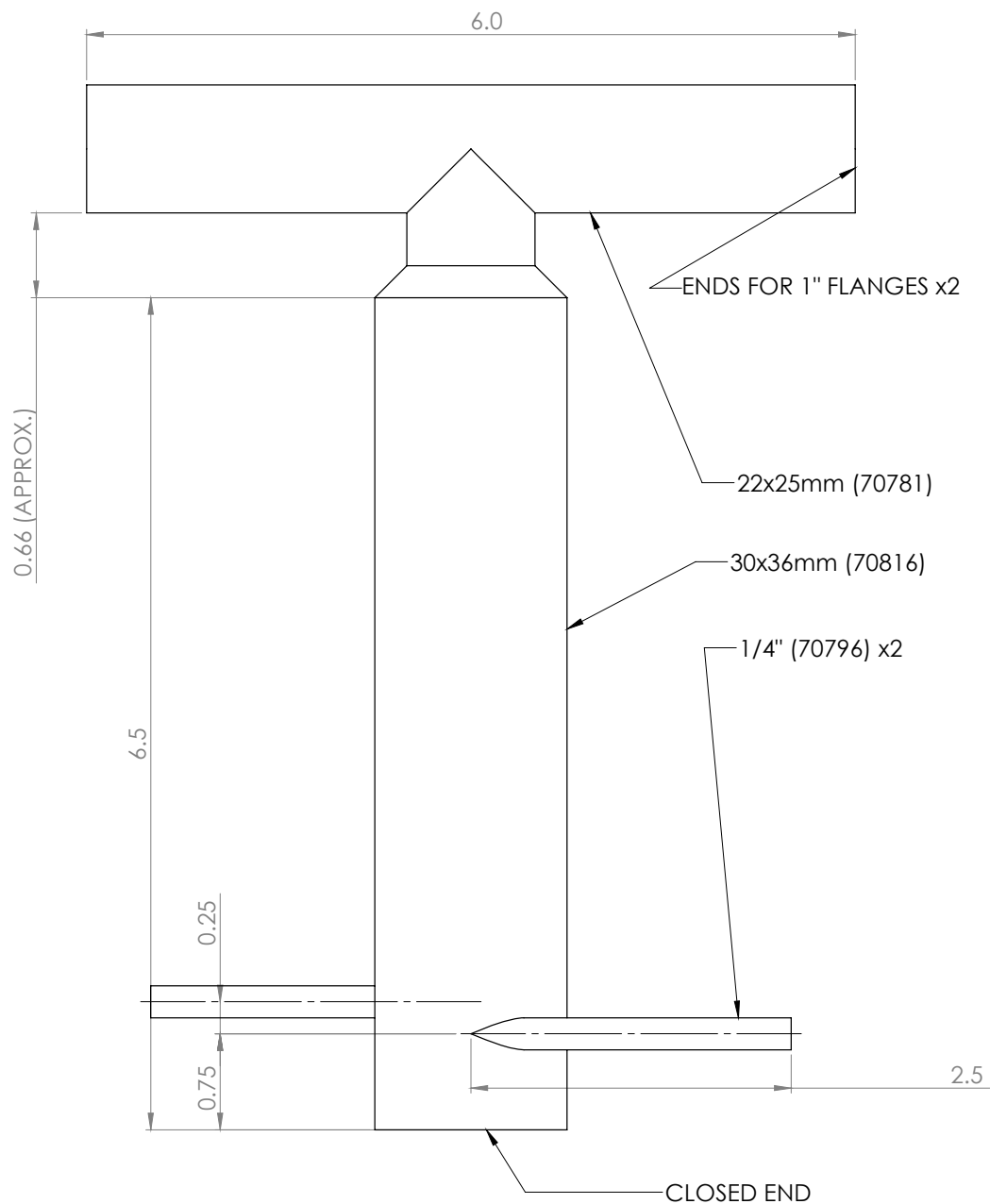


Figure A.1 Quartz ICP cell #1 engineering drawing, side view.

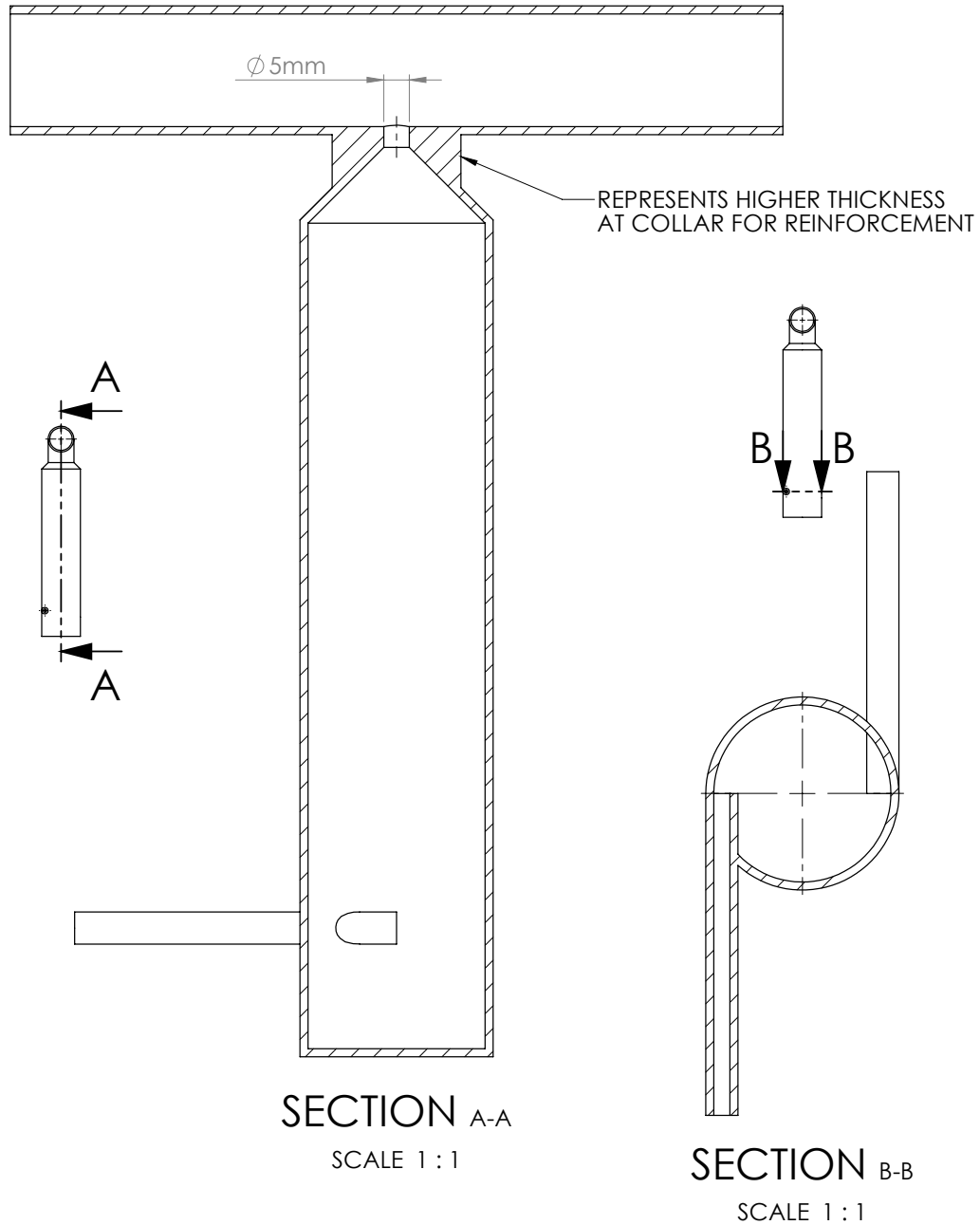


Figure A.2 Quartz ICP cell #1 engineering drawing, section view.

## Appendix B. Quartz ICP Cell #2 Engineering Drawings

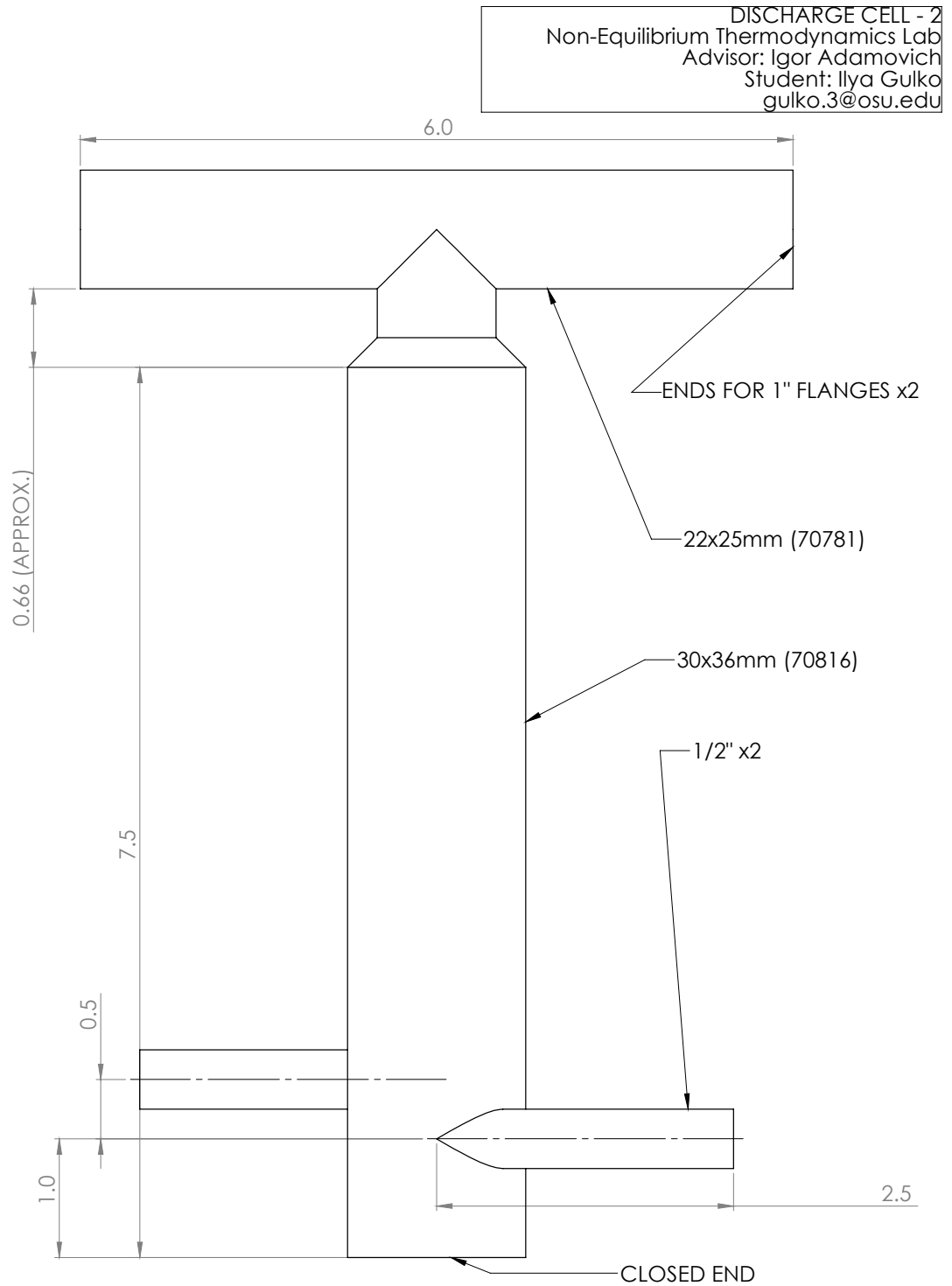


Figure B.1 Quartz ICP cell #2 engineering drawing, side view.



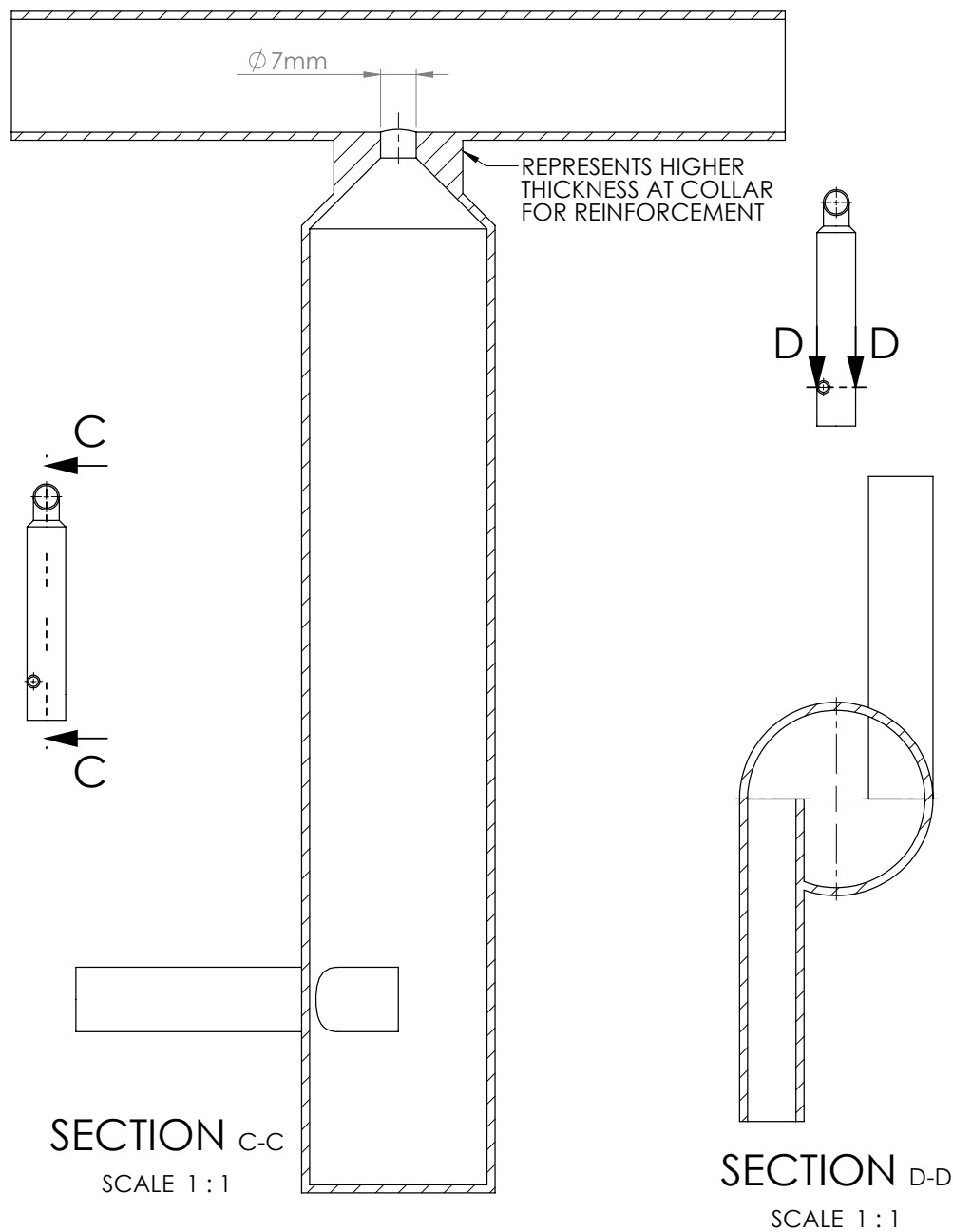


Figure B.2 Quartz ICP cell #2 engineering drawing, section view.

## Appendix C. Glass Observation Cell Engineering Drawing

ICP Observation Cell  
Non-Equilibrium Thermodynamics Lab  
Advisor: Igor Adamovich  
Student: Ilya Gulko  
gulko.3@osu.edu

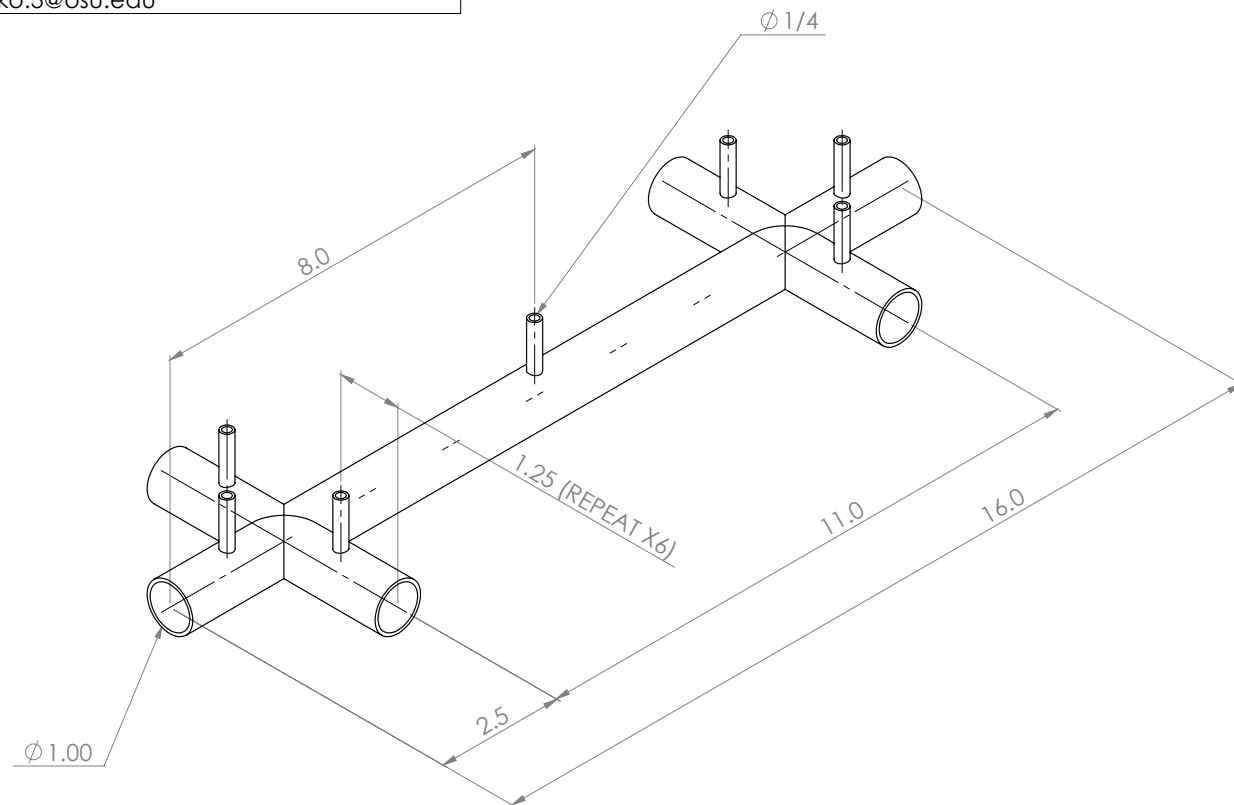


Figure C.1 Glass observation cell engineering drawing.